Development and validation of a one-dimensional transient rotodynamic pump model at component scale

Laura Matteo, Antoine Dazin, Nicolas Tauveron

Development and validation of a one-dimensional transient rotodynamic pump model at component scale

Laura Matteo[1], Antoine Dazin[2] and Nicolas Tauveron[3]

[1] CEA Université Paris-Saclay, DEN/DM2S/STMF, France
[2] LMFL FRE CNRS 2017, Arts et Métiers Paristech, Lille, France
[3] CEA Grenoble, DRT/LITEN/DTBH/SSETI, France

E-mail: laura.matteo@cea.fr

Abstract. For reactor design and safety purposes, the French Alternative Energies and Atomic Energy Commission (CEA) is currently working on the implementation of a predictive transient two-phase flow 4-quadrant rotodynamic pump model in the CATHARE-3 code (Code for Analysis of THermalhydraulics during an Accident of Reactor and safety Evaluation). This paper presents the pump model and its validation in single-phase first quadrant conditions at component scale. Explanations are first given on code architecture, meshing, equations to solve and how to switch from fixed frame to rotating frame and vice versa at impeller endpoints. Then, verification results in an ideal case are compared to Euler equations. Finally, validation results on real cases including the prediction of single-phase first quadrant steady performance curves and the simulation of a fast startup transient are presented.

1. Introduction to the project needs, methods and objectives

1.1. Industrial context and partners

For reactor design and safety purposes, the CEA is currently working on Sodium Fast Reactor (SFR) thermal-hydraulics [1]. A SFR is a system composed of three circuits (primary and secondary: liquid sodium and tertiary: gas nitrogen or water) and designed to both produce electricity and minimize nuclear waste generation. The primary circuit is composed of huge components such as primary pumps (figure 1), which play a great role in reactor transients dynamics. Hypothetic accidental transients like 'primary pump seizure' are studied using the CATHARE-3 code during the reactor design step. Throughout this type of transients, cavitation may occur in non-affected primary pumps and the affected pump may operate in reverse conditions in terms of flow rate and rotational speed.

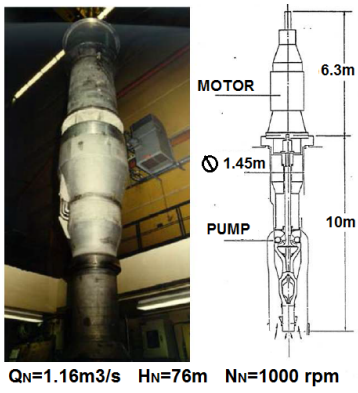

Figure 1. SFR primary pump (from Tauveron [2]).

However the primary pump 4-quadrant characteristics are not known at that moment as the pumps are still under design. For this purpose, CEA decided at the end of year 2015 to

implement a predictive transient, two-phase flow rotodynamic pump model in the CATHARE-3 code and to validate results at component scale (pump) and system scale (reactor) with respect to available experimental data. The model is called '1D-pump model' as a one-dimensional meshing is used to describe the pump from suction inlet to diffuser outlet. It is not only designed for sodium applications which explains that Framatome, ArianeGroup, CETIM and EDF industrial companies and LMFL lab support the project by providing data, funding or knowledge. Even if the subject of the 1D pump performance prediction is not new, some recent works are still investigating this field by proposing some improvements of the loss coefficients or slip factor correlations (Kara Omar et al 2017 [3], El Naggar 2013 [4], Ji et al 2010 [5]). Nevertheless most of this works are limited to steady operations and only few studies are proposing quantitative predictions of a pump during transient operations (Tanaka et Tsukamoto 1999 [6], Dazin et al 2007 [7]), and were only proposing a correction of the steady performance curve which is supposed to be known, by transient terms. Moreover, according to the authors' knowledge, most of the performance prediction models used in hydraulic system software are limited to the prediction of the pump operating in the normal pump quadrant, by the use of inlet/outlet velocity triangles based tools. The originality of the present project is to build a real 1D model -the mean streamline in the different parts of the pumps is meshed- able to predict the performance of mixed and radial flow pumps in purely liquid or gas/liquid, and four quadrant operations. The present paper is detailing the global strategy of this project and the results obtained on the first stage of this work which is focused on the transient performance of the pump in the 'normal pump' quadrant and single phase operation.

1.2. Development support: the CATHARE-3 code

CATHARE-3 is a french two-phase flow modular system code. It is owned and developped since 1979 by CEA and its partners EDF, Framatome and IRSN. See [8] for more details on the code development and validation strategy.

One-dimensional (1D), three-dimensional (3D) or point (0D) hydraulic elements can be associated together to represent a whole facility. They respectively correspond to one or three directions allowed for the fluid, and to components where fluid velocity is negligible such as capacities. Thermal and hydraulic submodules (as warming walls, valves, pumps, turbines...etc) can be added to main hydraulic elements to respectively take into account thermal transfer, flow limitation, pressure rise or pressure drop. Six local and instantaneous balance equations (mass, momentum and energy for each phase) make possible liquid and gas representation for transient calculations. Mechanical and thermal disequilibrium between phases can thus be represented [9]. Phase average imposes the use of physical closure laws in the balance equations system [10].

2. Description of the 1D pump developed model

2.1. The mean flow path

A blade-to-blade view (R-θ plane) of a centrifugal rotodynamic pump is shown on figure 2. Impeller blades define inter-blades channels where the fluid circulates. With a one-dimensional modelling, the definition of a mean flow path is needed (see figure 2). The case of mixed flow pumps can also be simulated by taking into account the tilt angle.

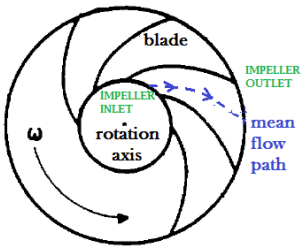

Figure 2. Centrifugal rotodynamic pump R-θ plane scheme.

2.2. 1D-pump code architecture

A two-phase flow one-dimensional transient model is used to model the pump. Each part of the pump (suction, impeller and diffuser) is meshed as shown on figure 3.

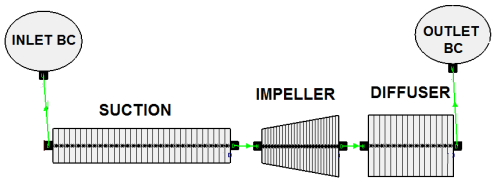

Figure 3. 1D-pump structure: three 1D elements.

This 1D mesh allows one direction for liquid and gas velocities but two possible ways (positive or negative).

2.3. Equations to solve

2.3.1. CATHARE-3 two-fluid model. For each part of the pump (fixed or rotating), a six local and instantaneous balance equations system (mass, momentum and energy for each phase) based on the CATHARE-3 bi-fluid model has been chosen.

It makes possible liquid and gas representation for transient calculations. By this way, mechanical and thermal disequilibrium between phases can be represented [9].

mass balance

$$\frac{\partial}{\partial t}A\alpha_k\rho_k + \frac{\partial}{\partial z}A\alpha_k\rho_k V_k = (-1)^k A\Gamma + S_k \tag{1}$$

momentum balance

$$\begin{aligned}\frac{\partial}{\partial t}A\alpha_k\rho_k V_k + \frac{\partial}{\partial z}A\alpha_k\rho_k V_k^2 + A\alpha_k\frac{\partial p}{\partial z} + Ap_i\frac{\partial \alpha_k}{\partial z}\\ +A\epsilon_k\beta\alpha(1-\alpha)\rho_m\left[\frac{\partial V_G}{\partial t} - \frac{\partial V_L}{\partial t} + V_G\frac{\partial V_G}{\partial z} - V_L\frac{\partial V_L}{\partial z}\right]\\ = A\epsilon_k\Gamma W_i - A\epsilon_k\tau_i - (C_k\chi_f + \frac{AK\alpha_k}{\partial z})\tau_k\\ +A\alpha_k\rho_k g_z + \frac{R(1-\alpha_k)}{4}p_i\frac{\partial A}{\partial z} + SM_k\end{aligned} \tag{2}$$

energy balance

$$\begin{aligned}\frac{\partial}{\partial t}\left[A\alpha_k\rho_k(h_k + \frac{V_k^2}{2})\right] + \frac{\partial}{\partial z}\left[A\alpha_k\rho_k V_k(h_k + \frac{V_k^2}{2})\right] - A\alpha_k\frac{\partial p}{\partial t}\\ = +A\alpha_k\rho_k V_k g_z + \chi_c q_{p,k} + Aq_{k,E} + A\epsilon_k\Gamma(h_k + \frac{W_i^2}{2}) + SE_k\end{aligned} \tag{3}$$

2.3.2. Summary of necessary adjunctions to CATHARE-3 bi-fluid model to represent a pump. Adapting CATHARE-3 to a rotating frame resolution in order to model a rotodynamic pump was a challenge and resulted in significant code developments. The following adjunctions or modifications to the standard CATHARE-3 1D-elements have been introduced to create a 1D-pump model, and especially to take into account the rotation effects:

- A centrifugal acceleration term has been added to balance equations of the impeller part.
- In the impeller, resolution is made with respect to the rotating frame.
- Section is calculated at impeller endpoints and inside impeller to solve equations with the relative velocity and ensure mass flow rate conservation at frame interfaces.
- Conservation of static pressure and static enthalpy is ensured at frame interfaces.
- At impeller outlet, acquired tangential dynamic pressure is converted into static pressure because only the streamwise velocity component is considered downstream to the impeller. In the next future, flow representation in the stator part (diffuser, volute) will be improved.
- A slip factor model (also called deviation in this paper) has been implemented.
- A desadaptation (shock) head loss source term has been added to momentum equations. For the moment, it is spread all along the impeller meshing but will probably be concentrated on impeller endpoints in the future.
- Power dissipation in the fluid due to low flow rate recirculations is added to energy equation.

Details on moving frame resolution, slip factor and losses models are respectively given in the following paragraphs 2.3.3, 2.3.4 and 2.3.5.

2.3.3. Focus on moving frame resolution. Inside impeller, resolution is made with respect to the rotating frame. W_k relative velocities are used in the impeller equations, unlike V_k absolute velocities are used in the pump fixed parts equations. When solving into a moving frame, entrainment accelerations have to be taken into account into momentum and energy equations. After projection of forces on the mean flow path, only centrifugal acceleration is involved and has to be added as a new source term to momentum and energy balance equations of each phase. Coriolis acceleration effect is taken into account by the deviation model (see 2.3.4). The expression of centrifugal acceleration is $\omega^2 R \frac{\partial R}{\partial z}$.

2.3.4. Deviation model. The mean flow path doesn't follow exactly the blade angle. At the nominal point, this phenomenon called deviation or slip reflects in a deviated outlet angle β_2' smaller than the outlet blade angle β_2. This is due to fluid relative circulation in the blade channels which is mainly due to the Coriolis acceleration. After reviewing some slip factor models developed in the last century (Stodola [11], Stanitz [12], Pfleiderer [13], Wiesner [14], Eck [15], Paeng and Chung [16], Ji [5], Qiu [17]), the Stodola one has been implemented in CATHARE-3 1D-pump model: $1 - \sigma = \frac{\pi sin(\beta_2)}{Z}$.

Although it is the first and oldest model, it is still mentionned and used as a reference in current studies [17]. It is simple to use and gives good results in our case (see figure 7). In the future of this project, other slip factor correlations will be tested with a largest validation basis including mixed-flow pumps.

2.3.5. Losses models. Several types of losses impact pump head generation. First, losses existing always in a classic pipe geometry (which existed in the CATHARE code before any 1D pump developments):

- Regular pressure loss term (wall friction): $C_k \chi_f \tau_k$
- Singular pressure loss term (abrupt section or direction change): $\frac{AK\alpha_k}{\partial z} \tau_k$

Second, losses specific to a rotodynamic pump (which were implemented in the CATHARE-3 code as part of 1D-pump developments):

- Desadaptation head loss (also called "Shock loss"): it has been introduced into momentum balance equations. At the pump design point, the relative flow is quite adapted to the blade leading edge angle at impeller inlet. When flow rate increases or decreases at a given rotational speed, flow desaptation inscreases. The corresponding head loss inscreases proportionally to $(Q - Q_{adapted})^2$ [18].
- Recirculation power loss (below the recirculation flow rate): it has been introduced into energy balance equations. It increases when flow rate decreases following an expotential form.

2.4. Required input data

Required input data can be separated into three types: general, geometric and hydraulic.

- General data: nominal point of the pump (Q_N, H_N, N_N). If rotational speed has to be computed by turning mass equation, then inertia, friction torque and synchronism velocity have to be provided.

- Geometric data: elements length, flow section evolution along fixed and mobile elements and orientation against vertical axis. For the impeller part: hub and tip radius and blade angles (β) at inlet and outlet, blades number.
- Hydraulic data: pressure, temperature and void fraction (at inlet boundary condition if needed).

3. Validation of steady performance curves

3.1. Objectives and method

In this section, two steps of comparison will be done on a centrifugal pump called DERAP, described in the following paragraph 3.2.

- A verification step: first, a theoretical verification is made by integrating 1D-pump model equations to obtain Euler head and torque expressions in ideal conditions associated to several hypothesis (see paragraph 3.3). Then, a comparison between DERAP 1D-pump ideal calculation results and Euler equations in which no deviation and no losses are taken into account is made. The aim is to check the validity of the model in a simple case.
- A validation step: a comparison between 1D-pump real calculation results and experimental performance curves for which deviation and losses models are activated is made.

Results of both comparisons are shown on the same head and torque graphs (figures 6 & 7).

3.2. Description of the studied pump: DERAP centrifugal pump

The DERAP pump has been set in Mechanical Laboratory of Lille (LMFL) to experiment cavitation phenomenon during pump fast startups. Single-phase and two-phase characteristics are available in the first operating quadrant for this pump [19]. Here only single-phase characteristics will be used to validate 1D-pump model results. DERAP impeller is shown on figures 4 and 5 below. After modelling DERAP using the CATHARE-3 1D-pump developed model, the pump data deck shown on figure 3 is obtained. Diffuser and volute have not been entirely modelled in this study. A more realistic representation will be done in the next future.

Geometric specifications	
Inlet vane angle (deg)	32.2
Outlet vane angle (deg)	23
Number of vanes	5
Inlet diameter D_1 (mm)	38.5
Outer diameter D_2 (mm)	202.5
Outer width b_2 (mm)	7

Figure 4. DERAP impeller picture and geometric specifications.

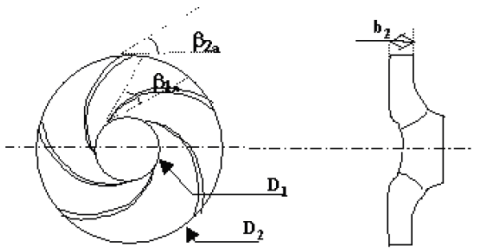

Figure 5. DERAP impeller scheme.

More information on DERAP pump geometric data is available in Duplaa [20]. DERAP specific speed value is 12.3 according to the common european definition of specific speed called N_{sq} (defined in [21]). DERAP nominal point is $Q_N = 23m^3/h$, $H_N = 50m$ and $N_N = 2900rpm$.

3.3. Theoretical verification: mathematical link between Euler and 1D-impeller equations.

Euler head and torque are obtained by applying the angular momentum theorem to a fluid volume inside an inter-blades channel [18]. The hypothesis applied to the 1D-pump model in order to correspond to Euler validity domain are the following: (H1) single-phase liquid

flow, (H2) steady regime, (H3) no hydraulic losses, (H4) adiabatic walls, (H5) no external mass or energy source or sink, (H6) gravitational acceleration neglected compared to centrifugal acceleration experienced by the fluid circulating in impeller.

With these hypothesis, the 1D-impeller system of equations is reduced to 3 equations with 3 unknown variables (mean pressure p, liquid mass enthalpy h_L and liquid relative velocity W_L). Euler head and torque expressions are found by integration of respectively 1D-impeller momentum and energy equations along curvilinear abscissa z.

3.4. Ideal and real 1D-pump model calculations: the transient defined to describe the 1st quadrant

To produce first quadrant head and torque 1D-pump model characteristics, a transient is defined keeping in mind that transient source terms have to stay negligible during calculation (transient has to be slow). First, rotational speed ω and flow rate Q are respectively initialized to zero and to $10\%Q_N$. Then rotational speed is linearly increased to nominal value ω_N. After stabilization at ω_N, flow rate is linearly increased to Q_N in a first step and increased again to $150\%Q_N$.

3.5. Ideal and real 1D-pump model results

Computation of the transient described above on DERAP 1D-pump modelling gives the following results. Figures 6 and 7 respectively show head versus flow rate (H-Q) and torque versus flow rate (C-Q) curves for Euler and 1D-pump ideal and real computations, and experimental performance characteristics from Duplaa [20] corresponding to 2900 rpm.

Ideal 1D-pump calculation and Euler head and torque curves are almost perfectly superimposed, what was the objective of the verification step. Then, concerning the validation step, deviation and losses models effects can be separately observed on each graph. Analyzing head characteristic on figure 6, it is still linear after taking account deviation but its slope has changed. The effect of regular losses is extremely low in this calculation, what could be anticipated because the real geometry of diffuser and volute has not been modelled yet. It should be observed at high flow rates. Shock losses effect can be seen on figure 6: it reduces head for off-design conditions. Remaining discrepancy between computed and experimental pump head performance could be attributed to: (1) A too simple modelling of the diffuser and volute geometry resulting in a underestimation of losses; (2) The effect of the DERAP pump significant leakage flow rate, that is not modelled yet. It would result in a offset in the performance characteristics (the flow rate measured experimentally is smaller than the effective flow rate inside impeller). These improvements in the modelling are currently undertaken.

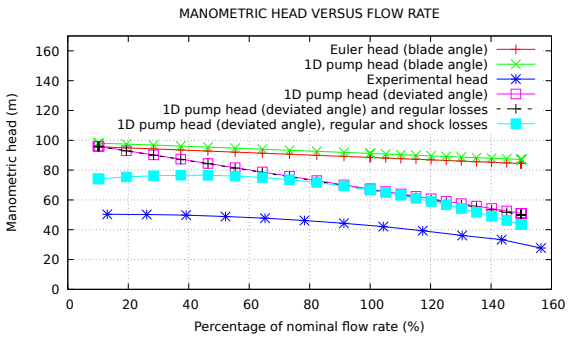

Figure 6. Validation of 1D pump ideal and real head prediction.

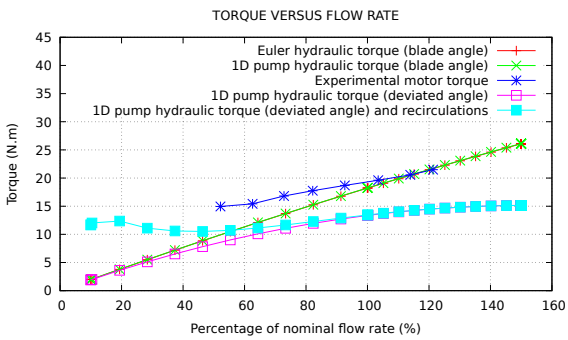

Figure 7. Validation of 1D pump ideal and real torque prediction.

The experimental torque drawn in figure 7 is a mechanical torque measured on the shaft: besides the hydraulic torque, it contains also the friction torque consumed by mechanical and disk friction as explained by Duplaa in [19], which are independent of flow rate (Stepanoff [18]). This explains a part of the offset existing between computed and experimental hydraulic torque. The modelling of the leakage flow rate could also reduce this gap. Torque results are nevertheless satisfactory because the slopes of experimental and calculated curves around the nominal point are similar. This is the effect of the deviation model. From this we can conclude that the slip factor from Stodola gives reasonable results in the flow rate studied range. At low flow rate, the torque consumed by recirculations can be observed when comparing to ideal perfomance curve.

One of the benefits of using such a 1D-pump model compared to a simpler Euler model is that pressure rise can be predicted on each mesh inside pump parts. Figure 8 represents the calculated pressure profile along the modelled suction, impeller and diffuser. The mean radius calculated by the 1D-pump model along the impeller can also be drawn (see figure 9). No experimental data are available to validate theses profiles for the DERAP pump but the pressure and mean radius profiles seem to have a shape in agreement with the physics of the flow.

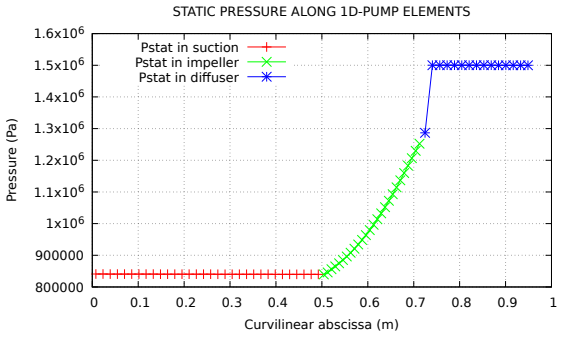

Figure 8. Pressure profile along pump elements (suction, impeller, diffuser).

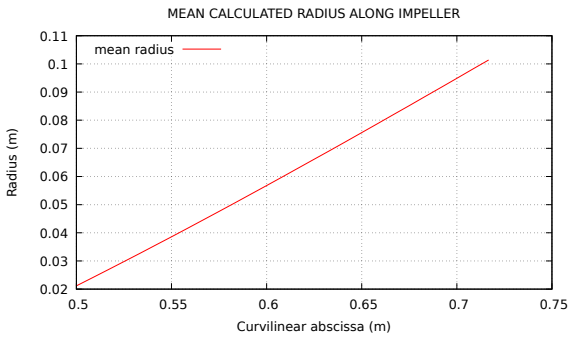

Figure 9. Calculated mean radius along impeller.

These verification and validation steps proved the validity of the 1D-pump model recently developed in the CATHARE-3 thermalhydraulic code. Head performance curve can be more precisely predicted by modelling the real geometry of diffuser and volute and by taking into account the flow rate leakage using an hydraulic link between impeller inlet and outlet. It is possible using the CATHARE-3 code. The prediction precision was not the priority of the present work, but it will be done in the future.

The CATHARE-3 1D-pump model will also be tested on pumps of various specific speeds and scales to complete the validation and improve models (in particular deviation and losses correlations). Indeed, DERAP is a rather small centrifugal pump with a very low specific speed and does not represent the behaviour of mixed-flow pumps used as primary pumps in nuclear reactors. But, one of the interests of studying DERAP is that some fast startup transients have been experimentally made at the LMFL. Such a transient will be simulated with the 1D-pump model in the following section.

4. Validation on a fast startup transient

DERAP startup transients are called "fast startups" because its rotational speed evolves from zero to approximately nominal speed in about one second. Time scales associated to these pump startups have been studied by Dazin [22]. Such a transient is simulated here after.

4.1. Objectives and method

The aim of the fast startup transient validation is to show the capacity of the CATHARE-3 1D-pump model to simulate transient calculations and not only predict steady performance curves.

Flow rate and rotational speed measured during experiment are imposed in the CATHARE-3 calculation and the aim is to predict the head rise as a function of time. The same deviation and losses models as in the previous steady validation part are used.

4.2. Startup transient results

Experimental flow rate is drawn on figure 10 as well as the flow rate imposed during calculation as a boundary condition at suction inlet. Experimental rotational speed and rotational speed imposed during calculation are also shown on figure 11. The curves are superimposed what proves that experimental conditions are well represented.

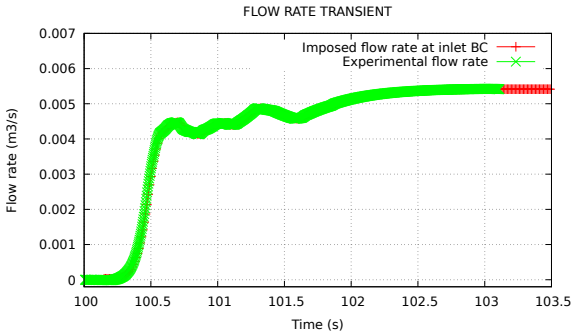

Figure 10. Flow rate during fast startup.

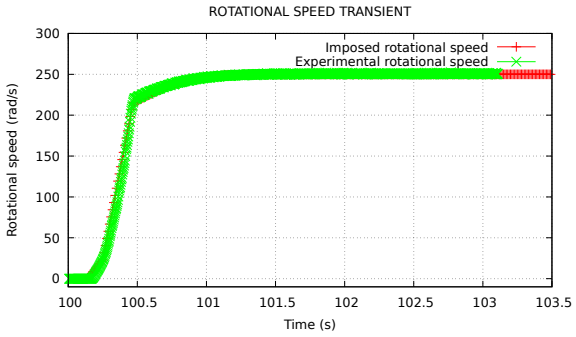

Figure 11. Rotational speed during fast startup.

Experimental and computed head rise is shown on figure 12. Computed torque rise is shown on figure 13 (no experimental data are available to validate this torque rise during the fast startup transient). Curves have been nondimensionalized with their value at the end of the transient. Only discrepancies associated to transient terms can thus be analyzed.

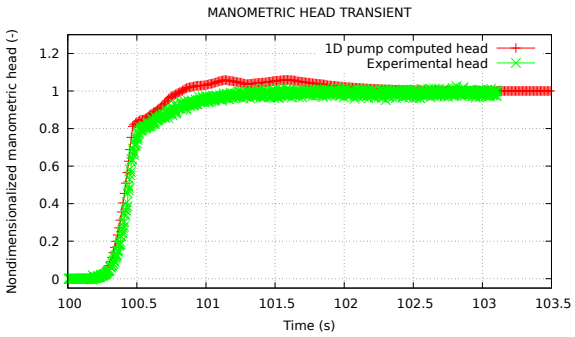

Figure 12. Head during fast startup.

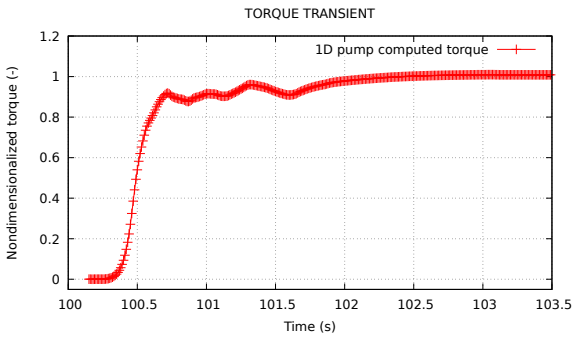

Figure 13. Torque during fast startup.

The obtained 1D-pump curves show the capacity of the model to simulate fast transients. These results are satisfactory as the difference between the experimental and modelled nondimensionalized head is less than 10% of the final value during the whole transient.

5. Conclusions and perspectives

A one-dimensional transient rotodynamic pump model is currently developped at the thermalhydraulic section of CEA Saclay (France). For the moment, first-quadrant single-phase performance characteristics can be predicted by this 1D-pump model and transient calculations can be managed. The present paper describes the 1D-pump model, explains the chosen way to first verify validity of model in an ideal case against Euler theory, validates the 1D-pump results against experimental pump performance characteristics and finally tests the capacity of the 1D-pump model to simulate fast transients such as 1-second pump startups.

Several further actions are scheduled to complete the 1D-pump development and validation. First, concerning DERAP, a more realistic geometry will be modelled to better take into account losses. A calculation using an hydraulic link between impeller inlet and outlet will be made to represent flow rate leakage. A similarity study will be managed by predicting DERAP performances at various rotational speeds. After this work, pumps of various specific speeds will be modelled to confirm verification and validation of the 1D-pump model in first-quadrant single-phase conditions. And then, developments and validation for two-phase flow and 4-quadrant conditions will be done. Concerning this, even if the validation has been done only in the first quadrant and in single-phase operation, it has to be noted that: first, the system of equations used to represent the pump is already adapted for two-phase flows, and second, the structure of the model needs only small modifications to allow reverse flow rate and rotational speed. Finally, system scale validation will be carried out on a setup representative of a primary circuit of a nuclear reactor.

Acknowledgments

Thanks to Framatome, ArianeGroup, CETIM and EDF industrial companies for supporting the project by providing data, funding or knowledge.

Nomenclature

Acronyms

Symbol	Description
$CATHARE$	Code for Analysis of THermalhydraulics during an Accident of Reactor and safety Evaluation
CEA	French Alternative Energies and Atomic Energy Commission
$CETIM$	CEntre Technique des Industries Mécaniques
EDF	Electricité De France
$IRSN$	Institut de Radioprotection et de Sûreté Nucléaire
$LMFL$	Laboratoire de Mécanique des Fluides de Lille
SFR	Sodium Fast Reactor

Subscripts

Symbol	Description
1	impeller inlet
2	impeller outlet
i	liquid-gas interface or ideal quantity
k	relative to k-phase (k=v or k=l)
l	liquid phase
N	nominal operating point
m	mean value
$stat$	static
v	gas phase

Greek letters

Symbol	Description
α	Void fraction
α_k	k-phase volumetric presence rate
β	Added mass coefficient or relative angle (between $-\vec{U}$ and $\vec{W}$)
Γ	Volumetric mass transfer
ϵ_k	$\epsilon_v = 1$ and $\epsilon_l = -1$
π	Angular constant ($= 180°$)
ρ	Density
ρ_k	k-phase density
ρ_m	Mean density $= \alpha\rho_G + (1-\alpha)\rho_L$
τ_i	Volumetric interfacial friction
σ	Slip factor
τ_k	Wall friction per unit of length
χ_c	Pipe heating perimeter
χ_f	Pipe rubbing perimeter
ω	Impeller rotational speed in rad/s
ω_s	Specific speed (definition different from N_s)

Latin letters

Symbol	Description
A	Flow section
b	Inter-blades channel thickness
C, C_k	Torque or k-phase friction coefficient
g_z	Gravitational acceleration projection on mean flow path
H	Manometric head
h_k	Mass enthalpy of phase k
N	rotational speed in rpm
N_s	Pump specific speed
p	Mean pressure on a mesh point
p_i	Interfacial pressure source term
Q	Volumetric flow rate
$q_{p,k}$	Wall heat transfert
$q_{k,E}$	Interfacial heat transfert
R	Stratification rate or mean radius in impeller
S_k	Phasic mass source
SE_k	Phasic energy source
SM_k	Phasic momentum source
t	Time
$\vec{U}$	Entrainment velocity vector
$\vec{V}$	Absolute velocity vector
V_k	k-phase velocity in fixed frame
$\vec{W}$	Relative velocity vector
W_k	k-phase velocity in mobile frame
W_i	Interfacial velocity
z	curvilinear abscissa
Z	Impeller blades number

References

[1] Chenaud M, Li S, Anderhuber M, Matteo L and Gerschenfeld A 2015 *NURETH-16* (Chicago USA)
[2] Tauveron N 2013 *Thermohydraulics simulations of transient and unstable phenomena in the turbomachine of the innovative nuclear reactors in a multiscale approach* (LMFA Lyon) Habilitation
[3] Kara-Omar A, Khaldi A and Ladouani A 2017 Prediction of centrifugal pump performance using energy loss analysis *Australian Journal of Mechanical Engineering* **15:3** 210–221
[4] El-Naggar M A 2013 A one-dimensional flow analysis for the prediction of centrifugal pump performance characteristics *International Journal of Rotating Machinery* **2013**
[5] Ji C, Zou J, Ruan X, Dario P and Fu X 2010 *Proc. IMechE* vol 225
[6] Tanaka T and Tsukamoto H 1999 Transient behaviour of a cavitating centrifugal pump at rapid change in operating conditions-part 3: Classifications of transient phenomena *Journal of Fluids Engineering* **121** 857–865
[7] Dazin A, Caignaert G and Bois G 2007 Transient behavior of turbomachineries: applications to radial flow pump startups *Journal of Fluids Engineering* **129**
[8] Barre F and Bernard M 1990 The CATHARE code strategy and assessment *Nuclear Engineering and Design* **124** 257–284
[9] Faydide B and Rousseau J 1980 *European Two Phase Flow Group Meeting* (Glasgow UK)
[10] Bestion D 1990 The physical closure laws in the CATHARE code *Nuclear Engineering and Design* **124** 229–245
[11] Stodola A 1927 *Steam and Gas Turbines* (McGraw-Hill New York)
[12] Stanitz J D 1952 Some theoretical aerodynamic investigations of impellers in radial and mixed-flow centrifugal compressors *Trans. ASME* **74** 473–497
[13] Pfleiderer C 1961 *Die Kreiselpumpen* (Springer-Verlag Berlin Gottingen Heidelberg)
[14] Wiesner F J 1967 A review of slip factors for centrifugal impellers *Journal of Engineering for Power* **89** 558–572
[15] Eck B 1972 *Ventilatoren* (Springer-Verlag Berlin Heidelberg New York)
[16] Paeng K and Chung M 2001 A new slip factor for centrifugal impellers *Proc. Institution of Mechanical Engineers, Part A* **215** 645–649
[17] Qiu X, Japikse D, Zhao J and Anderson M R 2011 Analysis and validation of a unified slip factor model for impellers at design and off-design conditions *Journal of Turbomachinery* **133** 1–10
[18] Stepanoff A J 1961 *Pompes centrifuges et pompes hélices* (Dunod)
[19] Duplaa S 2008 *Etude expérimentale du fonctionnement cavitant d'une pompe lors de séquences de démarrage rapide* Ph.D. thesis Arts et Métiers ParisTech
[20] Duplaa S, Coutier-Delgosha O, Dazin A, Roussette O, Bois G and Caignaert G 2010 Experimental study of a cavitating centrifugal pump during fast startups *Journal of Fluids Engineering* **132**
[21] Gülich J F 2014 *Centrifugal Pumps* (Springer)
[22] Dazin A, Caignert G and Dauphin-Tanguy G 2015 Model based analysis of the time scales associated to pump start-ups *Nuclear Engineering and Design* **293** 218–227